

## Measurement of the Casimir Force between Parallel Metallic Surfaces

G. Bressi,<sup>1</sup> G. Carugno,<sup>2</sup> R. Onofrio,<sup>2,3</sup> and G. Ruoso<sup>2,3,\*</sup>

<sup>1</sup>*INFN, Sezione di Pavia, Via Bassi 6, Pavia, Italy 27100*

<sup>2</sup>*INFN, Sezione di Padova, Via Marzolo 8, Padova, Italy 35131*

<sup>3</sup>*Dipartimento di Fisica 'G. Galilei', Università di Padova, Via Marzolo 8, Padova, Italy 35131*

(Received 10 October 2001; published 15 January 2002)

We report on the measurement of the Casimir force between conducting surfaces in a parallel configuration. The force is exerted between a silicon cantilever coated with chromium and a similar rigid surface and is detected by looking at the shifts induced in the cantilever frequency when the latter is approached. The scaling of the force with the distance between the surfaces was tested in the 0.5–3.0  $\mu\text{m}$  range, and the related force coefficient was determined at the 15% precision level.

DOI: 10.1103/PhysRevLett.88.041804

PACS numbers: 12.20.Fv, 04.80.Cc, 07.07.Mp

One of the most astonishing features of quantum physics is that, as an ultimate consequence of the uncertainty principle, the vacuum is not empty. The nontrivial structure of the quantum vacuum has profound implications at both the microscopic and macroscopic level. In particular, forces of extragravitational origin acting between neutral bodies have been predicted due to the deformation of vacuum fluctuations caused by the macroscopic boundary conditions. In recent years, a compelling motivation to better grasp the contribution of quantum vacuum to the space-time curvature [1–3] is provided by the reported evidence for an accelerating universe [4–6]. A first-principles calculation of the pressure due to zero-point electromagnetic fluctuations for the case of an indefinite plane cavity made of conducting materials spaced by a distance  $d$  is obtained by summing all the vacuum mode contributions [7]. This results in the prediction of the quantum vacuum pressure as  $P_C = K_C/d^4$ , where the coefficient  $K_C = \pi\hbar c/480 = 1.3 \times 10^{-27} \text{ N m}^2$  has been introduced, with  $\hbar$  and  $c$  denoting the Planck constant and the speed of light, respectively.

Several experimental attempts have been pursued during various decades for unambiguously verifying Casimir's prediction [8]. So far, this search has been successful only in a particular geometry, namely in a cavity constituted by a plane surface opposing a spherical one. Pioneering measurements by van Blokland and Overbeek [9] in such a configuration resulted in the observation of the associated Casimir force, and in its detailed comparison to the Lifshitz theory [10] taking into account finite conductivity effects. More recently, these measurements have been revived by using state-of-the-art torsion balances [11], atomic force microscopes [12], and high precision capacitance bridges [13]. The latter two experiments have reached 1% precision, more precise determinations being limited by the theoretical uncertainty due to the so-called proximity force theorem (see section 4.3 in [8] for details). Regarding the Casimir force between two parallel conducting surfaces, the situation originally discussed by Casimir, no clear experimental result has been obtained so far. The

only attempt in this configuration dates back to Sparnaay [14]. The experimental data he obtained “do not contradict Casimir's theoretical prediction” [14], but large systematic errors and uncontrollable electrostatic forces prevented a detailed quantitative study. In this Letter we report on the measurement of the Casimir force between parallel conducting surfaces in the 0.5–3.0  $\mu\text{m}$  range with 15% precision. Our results are expected to have far-reaching implications toward understanding the nature and role of quantum fluctuations at the macroscale, as well as for exploring gravity at the microscale.

In our experiment, the two parallel surfaces are the opposing faces of a cantilever beam, free to oscillate around its clamping point, and of another thicker beam rigidly connected to a frame with adjustable distance from the cantilever. Our apparatus has already been discussed in detail elsewhere [15], and a schematic of the experimental setup is shown in Fig. 1. We use a rectangularly shaped cantilever made of silicon (resistivity 10  $\Omega \text{ cm}$ ), with optically flat surfaces of size 1.9 cm  $\times$  1.2 mm  $\times$  47  $\mu\text{m}$  (average roughness  $\sim 10 \text{ nm}$ ), covered with a 50-nm-thick chromium layer. The resonator is clamped to a copper base by which it can be rotated around the horizontal axis, parallel to its faces, by using a nanometer step motor. The resonator is faced on one side by another silicon beam (hereafter called the source), placed along the orthogonal direction and also covered by a (thicker) chromium layer. This beam has the same longitudinal dimensions of the first one (1.9 cm  $\times$  1.2 mm) but is much thicker (0.5 mm). The source beam can be rotated by using step motors around the two axes complementary to the one controlled by the resonator tilting, thus providing fine control of the parallelism of the two opposing surfaces. The gap separation between the two surfaces is adjusted with a dc motor for the coarse movement, and finely tuned using a linear piezoelectric transducer (PZT) ceramic attached to the source. The source and the resonator are electrically connected to a voltage calibrator for the electrostatic calibrations or, alternatively, to an ac bridge for measuring the capacitance of the system. We detect the motion

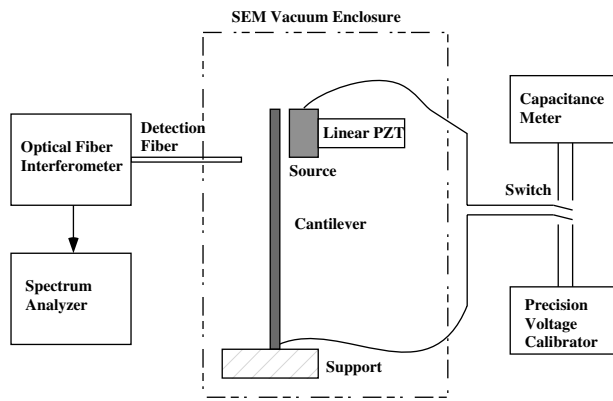


FIG. 1. Experimental setup. From left to right: displacement transducer, cantilever, and opposing surface (source) solidal to a PZT actuator, capacitance meter, and precision voltage source. The two opposing surfaces, on which the Casimir force is studied, form a capacitor with an area of  $1.2 \times 1.2 \text{ mm}^2$ . The source, the PZT, its support, and the motors are mechanically decoupled from the resonator by means of a set of alternated rubber rings and stainless steel disks. The apparatus is placed on the flange accessing the science chamber of a scanning electron microscope (SEM) Philips PSEM 500. This arrangement allows us to perform distance measurement and control the gap with a resolution up to 50–100 nm, as well as to work at a residual pressure of  $\sim 10^{-5}$  mbar, low enough to prevent direct acoustical pickup and to mitigate both the formation of oxide on metallic surfaces and the relocation on the gap of ambient dust present in the SEM.

of the resonator by means of a fiber optic interferometer [16] located on the opposite side of the resonator. The interferometer detects the relative displacement between the resonator and the detection fiber end, with a typical sensitivity of  $1.0 \times 10^{-7}$  m/V. The lowest torsional mode of the cantilever is monitored, its free frequency being  $\nu_0 = 138.275$  Hz and the mechanical quality factor  $\sim 10^3$ . The major problems, common to previous experimental efforts, are attributable to the difficulty to achieve and control the ideal conditions of parallel and neutral surfaces. The two surfaces must be kept parallel even at the smallest gaps investigated. Also, due to the presence of different metals in the electrical circuit connecting the two surfaces, an offset voltage  $V_0$  is always present in the gap, even when the two surfaces are nominally short circuited. This voltage prevents the possibility to obtain small gap separations because the electrostatic force will cause the resonator to attach to the source. For these reasons the measuring process can be divided into three stages: parallelization of the gap between the two surfaces, on-line estimate of the offset voltage  $V_0$ , and calibration with electrostatic fields, including one canceling the effect of  $V_0$  at leading order. This last stage allows one to reach the small separations ( $\leq 1 \mu\text{m}$ ) at which the Casimir force, thanks to its favorable scaling, is expected to dominate over the residual electrostatic force.

A prerequisite for the parallelization procedure is the stabilization and the elimination of dust particles present on the two surfaces. A  $\text{SiO}_2$  surface etching and the evaporation of a deposit of chromium provide stable metallic sur-

faces, and also prevents fast oxidation. For the cleaning, besides adopting standard procedures such as a dust-free laminar air flow environment able to filter powders of less than  $1 \mu\text{m}$ , and washing with proper solvents, we use a dedicated in-vacuum cleaning tool [15]. The latter is made of a thin metallic wire which, under inspection with the scanning electron microscope (SEM), is moved along three orthogonal axes through vacuum feedthroughs with micrometers. Dust grains of sizes between  $0.5$  and  $3 \mu\text{m}$ , difficult to identify under the optical microscope used for the preliminary, in air, cleaning, are then removed. Once the surfaces are cleaned at the  $0.5 \mu\text{m}$  level, we optimize their parallelism. A coarse arrangement is first done by using the SEM, i.e., viewing the gap at different magnifications on two orthogonal sides (see, for instance, Fig. 2). By means of the various motion controls it is possible to reach an almost parallel configuration (within a  $1 \mu\text{m}$  resolution). The final parallelism is then obtained using the ac bridge by maximizing the capacitance at the minimum obtainable gap separation. A maximum value of 22 pF is obtained, corresponding to an average gap separation of about  $0.4 \mu\text{m}$ . With an ac bridge sensitivity of  $\sim 0.4$  pF and based on the expression for the capacitance between nonparallel plates, this guarantees a parallelism better than 30 nm over 1.2 mm, equivalent to an angular deviation of  $\sim 3 \times 10^{-5}$  rad.

To control deviations from electrical neutrality of the two surfaces and to obtain a rough on-line determination of  $V_0$ , we measure the static deflection of the resonator versus the external voltage  $V_c$  applied with the calibrator

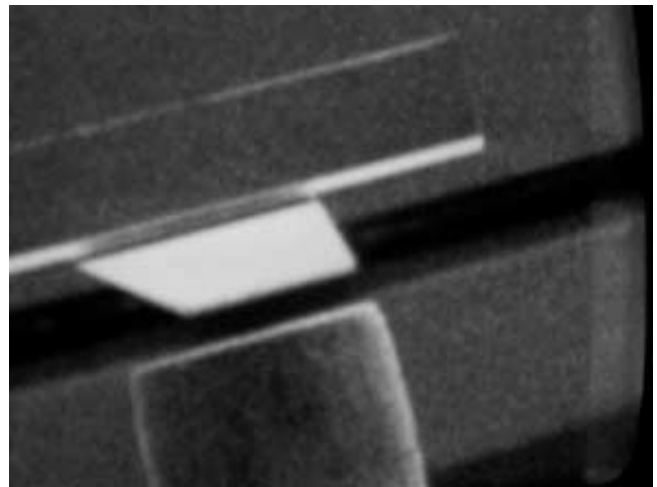


FIG. 2. Picture of the apparatus taken at the SEM. From top to bottom: source, cantilever, and detection fiber. The fiber is covered by a grounded conducting cylinder to prevent charging from the electrons emitted from the SEM, the latter being turned off during the data acquisition. During the measurement the fiber end is located within 20–50  $\mu\text{m}$  from the resonator. This distance range provides a trade-off between optimizing the visibility in the interference signal and avoiding the direct influence of the fiber end on the resonator-free frequency, e.g., due to residual charging. The field of view is  $3 \text{ mm} \times 2.3 \text{ mm}$ , and the gap is  $d = 110 \mu\text{m}$ .

for various gap distances  $d_i$ . The bending is measured by looking at the dc level of the fiber optic interferometer signal, and a repetitive procedure (by alternating bias voltages and zero voltage measurements) is adopted to cancel out the effect of drifts in the laser frequency. The static displacement  $\Delta x_i(V_c)$  of the resonator at its top edge is given by  $\Delta x_i(V_c) = K_i(V_c - V_0)^2$ . By fitting the measured data for each distance  $d_i$  with this law, we obtain an average value of  $V_0 = -(68.6 \pm 2.2)$  mV. The parameter  $K_i = \epsilon_0 S / 8\pi^2 m_{\text{eff}} \nu_0^2 d_i^2$  can also be used to evaluate the effective mass of the torsional mode, which is  $m_{\text{eff}} = (0.30 \pm 0.05)m_0$ , with  $m_0$  the physical mass, in agreement with theory [17].

By canceling the leading contribution of the offset voltage  $V_0$  through a counterbias voltage  $V_c \approx V_0$ , it is possible to look for distance-dependent forces superimposed to the residual bias  $V_r = V_c - V_0$ . This is done using a dynamical technique, i.e., by measuring the resonant frequency of the cantilever  $\nu$  as the gap separation is reduced. Any spatially dependent force is expected to induce a frequency shift whose sign is dependent on the attractive or repulsive nature of the force, negative frequency shifts signaling the presence of attractive forces. For a superposition of a residual electrostatic force contribution and the expected Casimir force the frequency shift is expressed as [15]

$$\Delta \nu^2(d) = \nu^2 - \nu_0^2 = -C_{\text{el}} \frac{V_r^2}{d^3} - \frac{C_{\text{Cas}}}{d^5}, \quad (1)$$

where  $C_{\text{el}} = \epsilon_0 S / 4\pi^2 m_{\text{eff}}$  and  $C_{\text{Cas}} = K_C S / \pi^2 m_{\text{eff}}$ , with  $\epsilon_0$  the vacuum dielectric constant,  $S$  the effective area delimited by the cantilever and the source surfaces, and  $m_{\text{eff}}$  the effective mass of the resonator mode [17].

In order to disentangle the two contributions on the right-hand side of Eq. (1), the measurements are performed in four situations differing by the applied bias voltage  $V_c$ . A delicate issue is the determination of the distance: all the measurements with variable gap are done by keeping the resonator fixed and moving the source by means of the linear ceramic PZT, always using increasing voltages to avoid hysteresis effects. The relative displacement between the source and the resonator is then expressed, in terms of the voltage  $V_{\text{PZT}}$  applied to the linear PZT, by  $d_r = d_r^0 - AV_{\text{PZT}} - d_s(V_{\text{PZT}})$ , where we have introduced the distance corresponding to  $V_{\text{PZT}} = 0$  V as  $d_r^0 = 1.2 \times 10^{-5}$  m, the actuation coefficient  $A = (1.508 \pm 0.002) \times 10^{-7}$  m/V, and  $d_s$  which takes into account the static deflection of the resonator due to the force. These last two quantities are measured with the fiber optic interferometer. The precision on the determination of  $d_r^0$  is very critical and we could not rely for its evaluation on the direct measurement at the SEM alone. For this reason the electrostatic calibration is also used to determine the correcting parameter  $d_0$ , such that  $d = d_r + d_0$  is the actual gap separation. Three out of the four measurements are done at large values of the bias voltage ( $V_c = [-205.8, -137.2, +68.6]$  mV) and large distances.

Figure 3 shows  $\Delta \nu^2$  versus the relative displacement  $d_r$ . The data are fitted with the function

$$\Delta \nu^2(d_r) = -\Delta \nu_{\text{offset}}^2 - C_{\text{el}} \frac{V_r^2}{(d_r + d_0)^3}, \quad (2)$$

where  $\Delta \nu_{\text{offset}}^2$  is a free frequency offset taking into account long term drifts. From a global fit we obtained the values  $\Delta \nu_{\text{offset}}^2 = (6 \pm 1)$  Hz<sup>2</sup>,  $d_0 = -(3.30 \pm 0.32) \times 10^{-7}$  m,  $C_{\text{el}} = (4.24 \pm 0.11) \times 10^{-13}$  Hz<sup>2</sup> m<sup>3</sup>, and  $V_0 = (60.2 \pm 1.7)$  mV, with a  $\chi^2$  probability of 85%.

It is now possible to analyze the data set for the fourth situation of bias voltage  $V_c = -68.6$  mV, corresponding to a quasicomplete cancellation of the effect of the offset voltage. From the acquired knowledge of the electrostatic component of the force we subtract its contribution and look at the residual frequency shift. The result is shown in Fig. 4 together with the best fit with the function

$$\Delta \nu^2(d) = -\frac{C_{\text{Cas}}}{d^5}. \quad (3)$$

This results in a value for the parameter  $C_{\text{Cas}} = (2.34 \pm 0.34) \times 10^{-28}$  Hz<sup>2</sup> m<sup>5</sup>, its sign confirming the expectation for an attractive force. A final check on the parallelism between the surfaces is done by fitting the data with a function taking into account a deviation from the plane parallel geometry [18]. The resulting deviation is  $0 \pm 30$  nm, in such a way that no change is observed for  $C_{\text{Cas}}$ , this confirming the value estimated in the parallelization procedure. From the definitions of  $C_{\text{el}}$  and  $C_{\text{Cas}}$  the coefficient of the Casimir force can be expressed as

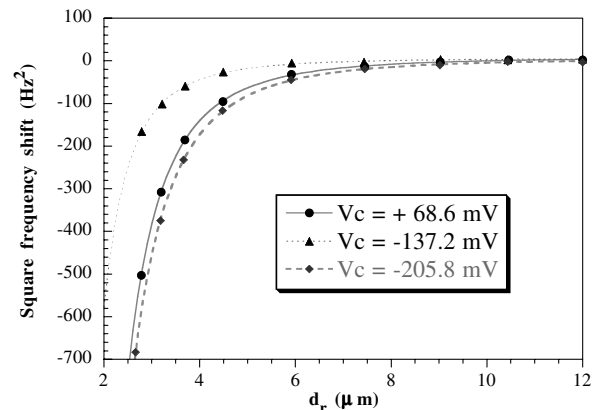


FIG. 3. Calibration with controllable electrostatic fields. The square frequency difference is shown versus distance for the three different values of the bias voltage  $V_c$ , as well as the fits with the electrostatic function [Eq. (2)]. Each frequency shift is evaluated through the fast-Fourier transform analyzer spectrum of the fiber interferometer signal (acquiring two rms averages with a resolution bandwidth of 31.25 mHz), which is then downloaded on a computer and fitted to a Lorentzian resonance curve to determine frequency and linewidth. The associated error arises from the Lorentzian fit plus a statistical uncertainty of 7 mHz. The overall acquisition time is kept below 40 min to minimize the drifts in the system, e.g., of thermal origin.

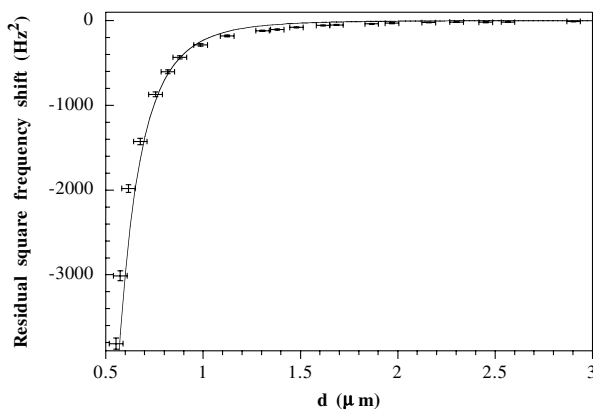


FIG. 4. Observation of the Casimir force. Residuals of the square frequency shift versus the gap distance and best fit with Eq. (3). The fit is done by considering the points at the nine smallest distances (0.5–1.1  $\mu\text{m}$  region), and includes the estimated errors, coming from the parameters  $C_{\text{el}}$ ,  $d_0$ , and  $V_0$ , both for the frequency shift and for the gap distance. The use of the nine points showing the largest shifts comes from a  $\chi^2$  analysis. With this choice the resulting  $\chi^2$  probability is 61%. A global fit also including a square frequency shift linearly increasing in time, with shift values ranging from 0 to 50  $\text{Hz}^2$ , allows for a possible explanation of the anomalous frequency shift evident in the 1–2  $\mu\text{m}$  region. This gives a force coefficient  $K_C = (1.24 \pm 0.10) \times 10^{-27} \text{Nm}^2$ , almost identical to the one previously found and with a  $\chi^2$  probability of 55%. Leaving the exponent of  $d$  as a free parameter leads to a best fit with exponent  $5.0 \pm 0.1$  as expected from the dynamical component of the Casimir force between parallel surfaces.

$$K_C = \frac{\epsilon_0}{4} \frac{C_{\text{Cas}}}{C_{\text{el}}} = (1.22 \pm 0.18) \times 10^{-27} \text{Nm}^2. \quad (4)$$

The value obtained agrees with the expected value of  $K_C$  first evaluated by Casimir [7]. It can be noted from Fig. 4 that the fitting curve does not describe systematically the experimental points in the 1–2  $\mu\text{m}$  region. There are, in principle, several conventional effects which could be invoked to explain the observed deviation (see also Fig. 4 caption), such as border effects, residual roughness of the surfaces, finite conductivity of chromium, or finite temperature corrections [8,19]. Work is in progress to refine the data analysis handling the Casimir term at a level necessary to further subtract its contribution from the data. The control of the Casimir force at this level and the evaluation of the residuals are necessary to test predictions, based on unification models of gravity to the electroweak and strong interactions, on new forces with intensity close to the gravitational force and acting below the millimeter range [20–22]. The parallel plate configuration maximizes the sensitivity to such forces [23,24], and could lead to stronger constraints than the one already evaluated from Casimir forces in the plane-sphere configuration [8].

Our experimental verification of the Casimir prediction for the force between two parallel conducting surfaces in the 0.5–3.0  $\mu\text{m}$  range leads to a measurement of the related coefficient with a 15 % precision. Our results

unambiguously show the existence of the quantum fluctuations at the macroscopic level, and confirm the existence of a delicate issue in matching quantum physics and the large scale evolution of the Universe via the cosmological constant problem. Furthermore, the technique demonstrated here and future refinements in various directions [15] could pave the road to high precision control of the Casimir forces crucial both for looking at new physics related to gravitation in the submillimeter range, as well as for designing electromechanical devices at the nanoscale.

We thank Z. Fontana for initial contributions to the experiment, F. Donadello, A. Galvani, and F. Veronese for skillful technical support, and L. Viola for a critical reading of the manuscript. The experiment was performed at the Laboratori Nazionali di Legnaro of the Istituto Nazionale di Fisica Nucleare.

\*Present address: INFN-LNL, via Romea 4, Legnaro, Italy 35020.

Email address: ruoso@lnl.infn.it

- [1] Y. B. Zeldovich, *Sov. Phys. JETP* **6**, 316 (1967).
- [2] S. Weinberg, *Rev. Mod. Phys.* **61**, 1 (1989); hep-ph/0005265.
- [3] E. Witten, hep-ph/0002297.
- [4] A. G. Riess *et al.*, *Astron. J.* **116**, 1009 (1998).
- [5] P. M. Garnavich *et al.*, *Astrophys. J.* **509**, 74 (1998).
- [6] S. Perlmutter *et al.*, *Astrophys. J.* **517**, 565 (1999).
- [7] H. B. G. Casimir, *Koninkl. Ned. Akad. Wetenschap. Proc* **51**, 793 (1948).
- [8] M. Bordag, U. Mohideen, and V. M. Mostepanenko, *Phys. Rep.* **353**, 1 (2001).
- [9] P. H. G. M van Blokland and J. T. G. Overbeek, *J. Chem. Soc. Faraday Trans. I* **74**, 2637 (1978).
- [10] E. M. Lifshits, *Sov. Phys. JETP* **2**, 73 (1956).
- [11] S. K. Lamoreaux, *Phys. Rev. Lett.* **78**, 5 (1997).
- [12] U. Mohideen and A. Roy, *Phys. Rev. Lett.* **81**, 4549 (1998); B. W. Harris, F. Chen, and U. Mohideen, *Phys. Rev. A* **62**, 052109 (2000).
- [13] H. B. Chan *et al.*, *Science* **291**, 1941 (2001).
- [14] M. J. Sparnaay, *Physica (Utrecht)* **24**, 751 (1958).
- [15] G. Bressi *et al.*, *Classical Quantum Gravity* **18**, 3943 (2001).
- [16] D. Rugar, H. J. Marmin, and P. Guethner, *Appl. Phys. Lett.* **55**, 2588 (1989).
- [17] J. E. Sader *et al.*, *Rev. Sci. Instrum.* **66**, 3789 (1995).
- [18] M. Bordag, G. L. Klimchitskaya, and V. M. Mostepanenko, *Int. J. Mod. Phys. A* **10**, 2661 (1995).
- [19] A. Lambrecht and S. Reynaud, *Eur. Phys. J. D* **8**, 309 (2000).
- [20] E. Fischbach and C. Talmadge, *The Search for Non Newtonian Gravity* (Springer-Verlag, Berlin, 1999).
- [21] I. Antoniadis, S. Dimopoulos, and G. Dvali, *Nucl. Phys.* **B516**, 70 (1998).
- [22] N. Arkani-Hamed, S. Dimopoulos, and G. Dvali, *Phys. Rev. D* **59**, 086004 (1999).
- [23] G. Carugno *et al.*, *Phys. Rev. D* **55**, 6591 (1997).
- [24] J. C. Long, H. W. Chan, and J. C. Price, *Nucl. Phys.* **B539**, 23 (1999).